

Thermoelectric properties of skutterudites $\text{Fe}_x\text{Ni}_y\text{Co}_{1-x-y}\text{Sb}_3$ ($x = y$)

J.L. Mi^a, X.B. Zhao^{a,*}, T.J. Zhu^a, J. Ma^b

^a State Key Laboratory of Silicon Materials, Department of Materials Science and Engineering, Zhejiang University, Hangzhou 310027, China

^b School of Materials Science and Engineering, Nanyang Technological University, 639798 Singapore, Singapore

Received 23 September 2006; received in revised form 9 November 2006; accepted 10 November 2006

Available online 4 December 2006

Abstract

Thermoelectric properties of skutterudites $\text{Fe}_x\text{Ni}_y\text{Co}_{1-x-y}\text{Sb}_3$ ($x = y = 0, 0.125, 0.25, 0.33, 0.375$) have been reported. $\text{Fe}_x\text{Ni}_y\text{Co}_{1-x-y}\text{Sb}_3$ compounds were synthesized by direct reactions between the elements. Both p-type and n-type thermoelectric materials can be obtained in $\text{Fe}_x\text{Ni}_y\text{Co}_{1-x-y}\text{Sb}_3$ system. The electrical conductivity measurements showed typical semiconductor behavior. The values of thermal conductivity at room temperature were substantially reduced from 9 to $3 \text{ W m}^{-1} \text{ K}^{-1}$ by the substitution of Fe and Ni for Co in CoSb_3 . The highest figure of merit (ZT) of 0.16 is obtained for $\text{Fe}_{0.375}\text{Ni}_{0.375}\text{Co}_{0.25}\text{Sb}_3$ at 610 K.

© 2006 Elsevier B.V. All rights reserved.

Keywords: Skutterudite; $\text{Fe}_x\text{Ni}_y\text{Co}_{1-x-y}\text{Sb}_3$; Thermal conductivity; Thermoelectric properties

1. Introduction

Compounds with skutterudite structure have been studied extensively since they were reported as potential novel thermoelectric materials at elevated temperatures [1–5]. The efficiency of thermoelectric materials can be characterized by the dimensionless figure of merit $ZT = (\alpha^2 \sigma / \kappa) T$, where α is the Seebeck coefficient, σ and κ are the electrical and thermal conductivity, respectively, and T is Kelvin temperature. Most binary skutterudite compounds possess large Seebeck coefficient and good electrical conductivity. However, their thermal conductivity is too high to make them useful for the application in thermoelectric devices. Compared to state-of-the-art thermoelectric materials, the room temperature thermal conductivity of binary skutterudites ($10\text{--}15 \text{ W m}^{-1} \text{ K}^{-1}$) is too high to result in high figures of merit [6]. Synthesizing filled skutterudites, which are supposed as the “phonon-glass/electron-crystal” materials, is an efficient solution to reduce the lattice thermal conductivity. The “rattling” motion of the filling atoms strongly scatters phonons and causes a significant decrease of the lattice thermal conductivity and hence an increase of the figure of merit [7].

Another important feature of skutterudite materials is the large number of different isostructural compositions that can

be synthesized [8–11]. The formation of solid solutions with isostructural compounds is another powerful approach to achieve a lower thermal conductivity by increasing the point defect scattering. The preparation and thermoelectric properties of skutterudite-related phase $\text{Ru}_{0.5}\text{Pd}_{0.5}\text{Sb}_3$ have been studied [8] and the results have shown that the lattice thermal conductivity is substantially lower than that of the binary compounds CoSb_3 and IrSb_3 . The lattice contribution to the thermal conductivity is greatly reduced in other ternary compounds such as $\text{Fe}_{0.5}\text{Ni}_{0.5}\text{Sb}_3$ and $\text{IrSn}_{1.5}\text{Se}_{1.5}$, with room temperature values ranging from 1.5 to $3 \text{ W m}^{-1} \text{ K}^{-1}$ [10]. The phase constitution and the Seebeck coefficient at room temperature of quaternary $\text{Fe}_x\text{Co}_y\text{Ni}_z\text{Sb}_{24}$ ($x + y + z = 8$) have been investigated [12]. Partial solid solutions were suggested in $\text{CoSb}_3\text{--Fe}_{0.5}\text{Ni}_{0.5}\text{Sb}_3$ system, and a phonon thermal conductivity of $3.5 \text{ W m}^{-1} \text{ K}^{-1}$ was obtained for $(\text{CoSb}_3)_{0.79}\text{--}(\text{Fe}_{0.5}\text{Ni}_{0.5}\text{Sb}_3)_{0.21}$ [13]. For a further study of $\text{CoSb}_3\text{--Fe}_{0.5}\text{Ni}_{0.5}\text{Sb}_3$ system, quaternary solid solutions with different compositions $\text{Fe}_x\text{Ni}_y\text{Co}_{1-x-y}\text{Sb}_3$ ($x = y = 0, 0.125, 0.25, 0.33, 0.375$) have been prepared and their thermoelectric properties are presented in this investigation.

2. Experimental

$\text{Fe}_x\text{Ni}_y\text{Co}_{1-x-y}\text{Sb}_3$ ($x = y = 0, 0.125, 0.25, 0.33, 0.375$) compounds were synthesized by the reactions between the elements under vacuum in silica tubes. Stoichiometric amounts of Fe (99.5%), Co (99.9%), Ni (99.9%) and Sb (99.5%)

* Corresponding author. Fax: +86 571 87951451.

E-mail address: zhaoxb@zju.edu.cn (X.B. Zhao).

shots were sealed in the evacuated amorphous carbon-coated quartz ampoules. After melting at 1373 K for 20 h, the ampoules were quenched in water. The products were then ground into powders, pressed into dense cylindrical pellets and loaded in a second quartz ampoule and annealed under vacuum at 973 K for 100 h to form the correct crystallographic phase. After the heat treatment, the products were ground into powder again and hot pressed at 823 K for 30 min under a pressure of 50 MPa.

The samples were analyzed with X-ray diffraction (XRD) on a RigakuD/MAX-2550PC diffractometer using Cu K α radiation ($\lambda = 1.5406 \text{ \AA}$) in the range of $2\theta = 20\text{--}80^\circ$. The electrical conductivity and Seebeck coefficient were measured at a computer-assistant device. The electrical conductivity σ was obtained by a four-probe method. For the measurement of Seebeck coefficient α , one end of the sample was heated to produce a temperature difference between both ends of the sample up to about 5°C , when the thermoelectric power ΔU and temperature difference ΔT were simultaneously measured by an Agilent 34401A Multimeter. The Seebeck coefficient was then obtained by the slope of $\Delta U/\Delta T$ calculated from more than 50 pairs of ΔU and ΔT at each measuring temperature. The thermal conductivity κ was calculated by $\kappa = aC_p d$, where d is the material density was measured by Archimedes method at room temperature, a the thermal diffusivity measured by a Netzsch LFA 427 laser flash apparatus, and C_p is the specific heat capacity measured by Netzsch DSC 404 and fitted with a cubic polynomial to calculate the C_p at the same temperature of thermal diffusivity. For the calculation of the power factor $\alpha^2\sigma$ and the dimensionless figure of merit $ZT = (\alpha^2\sigma/\kappa)T$, α and κ were fitted with cubic polynomials.

3. Results and discussion

Fig. 1(a) shows the powder XRD pattern of sample $\text{Fe}_{0.25}\text{Ni}_{0.25}\text{Co}_{0.5}\text{Sb}_3$ after melting, and Fig. 1(b) gives the powder XRD patterns of $\text{Fe}_x\text{Ni}_y\text{Co}_{1-x-y}\text{Sb}_3$ ($x=y=0, 0.125, 0.25, 0.33, 0.375$) after annealing at 973 K for 100 h. The as-melted alloy exhibited double-phased structure with the phases of Sb and MSb_2 ($M = \text{Fe, Ni, Co}$), but the skutterudite phase was not found. It is because the kinetic process of the peritectic reaction is too slow to form skutterudite phase. As shown in Fig. 1(b), after annealing at 973 K for 100 h, only the skutterudite-related phase was found and other phases disappeared. The major peaks of the patterns for all samples can be indexed to the skutterudite structure with the space group of $Im\bar{3}$ according to JCPDS 76-0470. It can be concluded that the exact skutterudite phase is formed after sufficient solid-state reactions during annealing.

Lattice parameters for $\text{Fe}_x\text{Ni}_y\text{Co}_{1-x-y}\text{Sb}_3$ ($x=y=0, 0.125, 0.25, 0.33, 0.375$) derived from the XRD patterns were plotted in Fig. 2 versus the substituting fraction of Fe and Ni. The lattice parameter a of CoSb_3 obtained in the present work is 9.0362 \AA , very close to the standard value of 9.034 \AA according to JCPDS 76-0470. A linear relationship between the lattice parameters and the substituting fractions from CoSb_3 to $\text{Fe}_{0.375}\text{Ni}_{0.375}\text{Co}_{0.25}\text{Sb}_3$ can be seen from Fig. 2. The linear relationship can be further extended to $\text{Fe}_{0.5}\text{Ni}_{0.5}\text{Sb}_3$ using the data reported in Refs. [10,13]. This suggests that a single phase solid solution should exist at least in the substituting range of our work of $0 < x = y < 0.375$.

Fig. 3 presents the temperature dependences of Seebeck coefficient for $\text{Fe}_x\text{Ni}_y\text{Co}_{1-x-y}\text{Sb}_3$ from room temperature to about 700 K. CoSb_3 and $\text{Fe}_{0.25}\text{Ni}_{0.25}\text{Co}_{0.5}\text{Sb}_3$ show p-type conduction as they have positive Seebeck coefficients, while $\text{Fe}_{0.125}\text{Ni}_{0.125}\text{Co}_{0.75}\text{Sb}_3$, $\text{Fe}_{0.33}\text{Ni}_{0.33}\text{Co}_{0.34}\text{Sb}_3$, $\text{Fe}_{0.375}\text{Ni}_{0.375}\text{Co}_{0.25}\text{Sb}_3$ exhibit n-type conduction with negative Seebeck coefficients. Undoped CoSb_3 is intrinsically p-type [14].

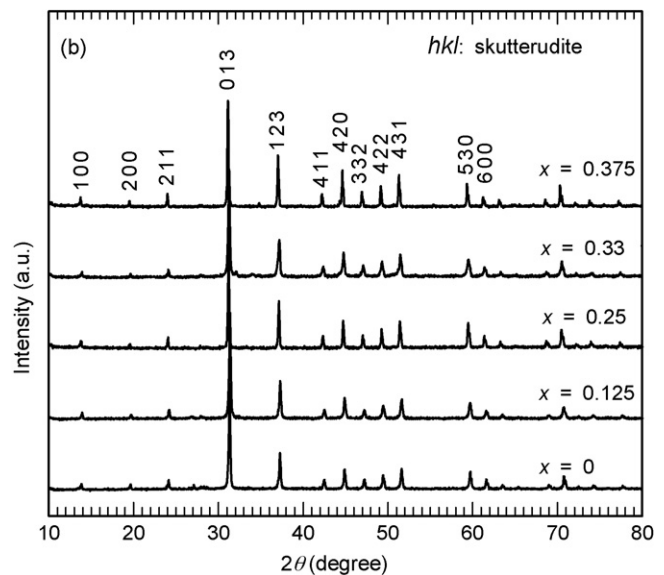
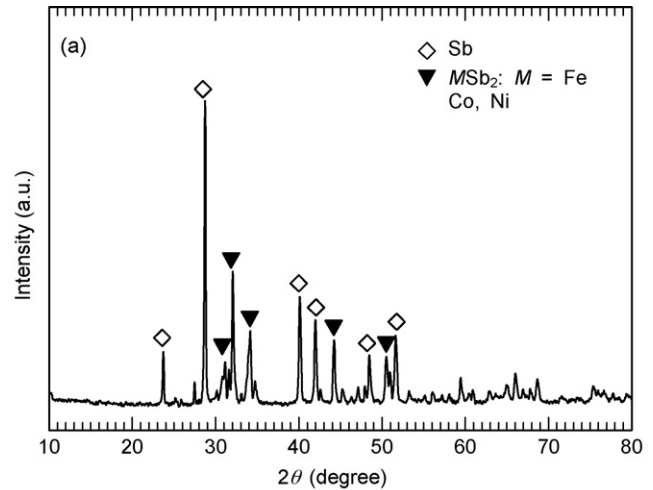


Fig. 1. XRD patterns of $\text{Fe}_{0.25}\text{Ni}_{0.25}\text{Co}_{0.5}\text{Sb}_3$ after melting (a) and of $\text{Fe}_x\text{Ni}_y\text{Co}_{1-x-y}\text{Sb}_3$ ($x=y=0, 0.125, 0.25, 0.33, 0.375$) after annealing (b).

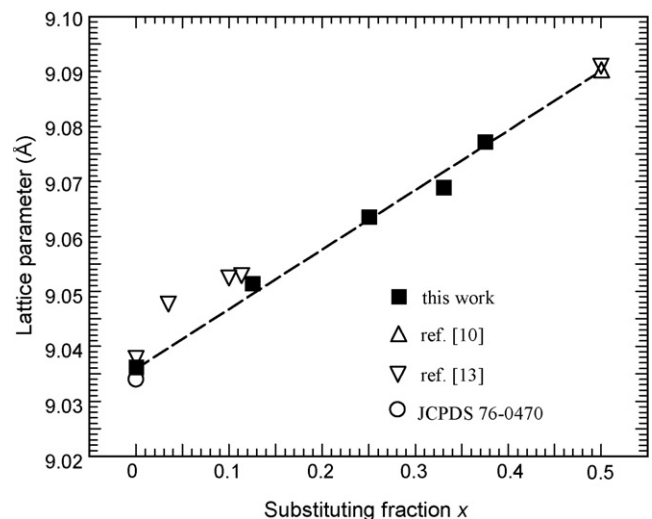


Fig. 2. Lattice constant as a function of x for $\text{Fe}_x\text{Ni}_y\text{Co}_{1-x-y}\text{Sb}_3$ ($x=y=0, 0.125, 0.25, 0.33, 0.375$).

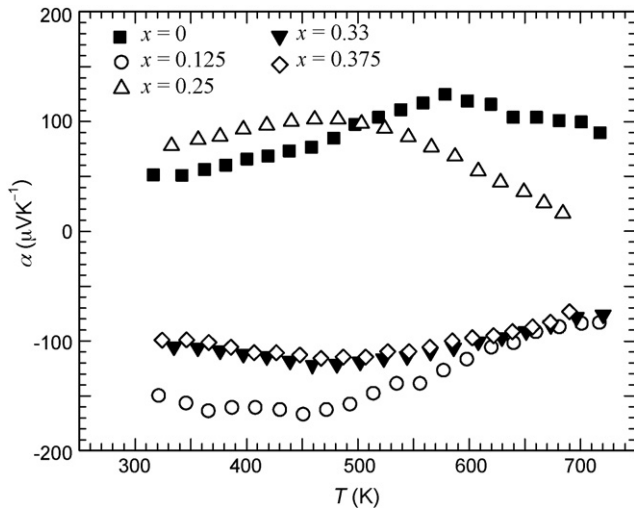


Fig. 3. Temperature dependences of Seebeck coefficient α for $\text{Fe}_x\text{Ni}_y\text{Co}_{1-x-y}\text{Sb}_3$.

It can be noted that $\text{Fe}_x\text{Ni}_y\text{Co}_{1-x-y}\text{Sb}_3$ system can provide both p-type and n-type thermoelectric materials by the deviation from the stoichiometric compositions. The p-type conduction of $\text{Fe}_{0.25}\text{Ni}_{0.25}\text{Co}_{0.5}\text{Sb}_3$ might be because the sample contains more Fe than Ni, and n-type conduction for $x=0.125, 0.33$ and 0.375 are attributed to a smaller Fe content than Ni. It is possible for Fe and Ni substituted CoSb_3 to behave both p-type and n-type conduction. Hasaka et al. [15] reported a homogeneity range of $0.45 < x < 0.55$ in $\text{Fe}_{1-x}\text{Ni}_x\text{Sb}_3$ and the conduction was p-type for $x < 0.5$ and n-type for $x > 0.5$. This is an advantage for the design of π -type thermoelectric elements. For all the samples, the absolute values of α increase with temperature, reach a maximum value at the certain temperature, and start to decrease at the higher temperatures. This is mainly ascribed to the occurrence of an increasing number of thermally excited minority carriers at higher temperatures, which tends to decrease the Seebeck coefficient. The highest absolute value of Seebeck coefficient is $165 \mu\text{V K}^{-1}$ obtained at about 450 K for $\text{Fe}_{0.125}\text{Ni}_{0.125}\text{Co}_{0.75}\text{Sb}_3$.

The temperature dependences of electrical conductivity σ of the samples are shown in Fig. 4. The electrical conductivity of all the samples increases with temperature over the measured temperature range, indicating the semiconductor behavior. The electrical conductivity increases with Fe and Ni substitution except CoSb_3 , and $\text{Fe}_{0.375}\text{Ni}_{0.375}\text{Co}_{0.25}\text{Sb}_3$ shows the highest electrical conductivity of $80,000 \Omega^{-1} \text{m}^{-1}$ at 700 K. The values of electrical conductivity of n-type $\text{Fe}_{0.125}\text{Ni}_{0.125}\text{Co}_{0.75}\text{Sb}_3$ and p-type $\text{Fe}_{0.25}\text{Ni}_{0.25}\text{Co}_{0.5}\text{Sb}_3$ are at the same level, but n-type $\text{Fe}_{0.125}\text{Ni}_{0.125}\text{Co}_{0.75}\text{Sb}_3$ shows the higher absolute values of Seebeck coefficient. While n-type $\text{Fe}_{0.33}\text{Ni}_{0.33}\text{Co}_{0.34}\text{Sb}_3$ and $\text{Fe}_{0.375}\text{Ni}_{0.375}\text{Co}_{0.25}\text{Sb}_3$ show even higher electrical conductivity with little higher absolute values of Seebeck coefficient. In general, Seebeck coefficient increases with the decreasing carrier concentration, but increases with increasing carrier effective mass. This implies that the electron effective mass of n-type samples are larger than the hole effective mass of p-type ones, which is consistent with the previous report [10].

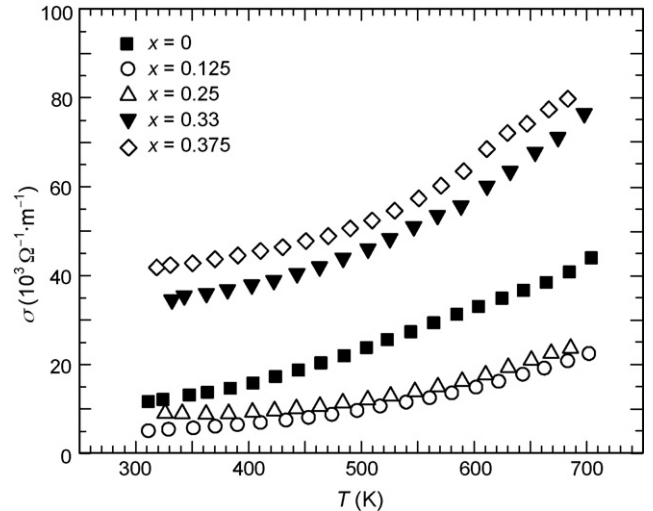


Fig. 4. Temperature dependences of electrical conductivity σ for $\text{Fe}_x\text{Ni}_y\text{Co}_{1-x-y}\text{Sb}_3$.

Fig. 5 shows the power factor ($\alpha^2\sigma$) of the $\text{Fe}_x\text{Ni}_y\text{Co}_{1-x-y}\text{Sb}_3$ compounds as a function of temperature. $\text{Fe}_{0.33}\text{Ni}_{0.33}\text{Co}_{0.34}\text{Sb}_3$ and $\text{Fe}_{0.375}\text{Ni}_{0.375}\text{Co}_{0.25}\text{Sb}_3$ show much higher power factor values than other samples. A highest power factor of $6.6 \times 10^{-4} \text{W m}^{-1} \text{K}^{-2}$ is obtained at about 550 K for $\text{Fe}_{0.375}\text{Ni}_{0.375}\text{Co}_{0.25}\text{Sb}_3$. It is desirable to adjust the carrier concentrations in the $\text{Fe}_x\text{Ni}_y\text{Co}_{1-x-y}\text{Sb}_3$ system by shifting the equilibrium Fe/Ni ratio to improve the thermoelectric properties without increasing markedly the thermal conductivity.

Fig. 6 shows the temperature dependences of thermal conductivity of CoSb_3 , $\text{Fe}_{0.25}\text{Ni}_{0.25}\text{Co}_{0.5}\text{Sb}_3$ and $\text{Fe}_{0.375}\text{Ni}_{0.375}\text{Co}_{0.25}\text{Sb}_3$. As can be seen, both quaternary skutterudites $\text{Fe}_{0.25}\text{Ni}_{0.25}\text{Co}_{0.5}\text{Sb}_3$ and $\text{Fe}_{0.375}\text{Ni}_{0.375}\text{Co}_{0.25}\text{Sb}_3$ have much lower κ than that of binary CoSb_3 . The values of thermal conductivity between the two quaternary samples are nearly the same, about $3 \text{W m}^{-1} \text{K}^{-1}$ at room temperature, which are substantially reduced from about $9 \text{W m}^{-1} \text{K}^{-1}$ for CoSb_3 . The total thermal conductivity κ of a material consists of the phonon

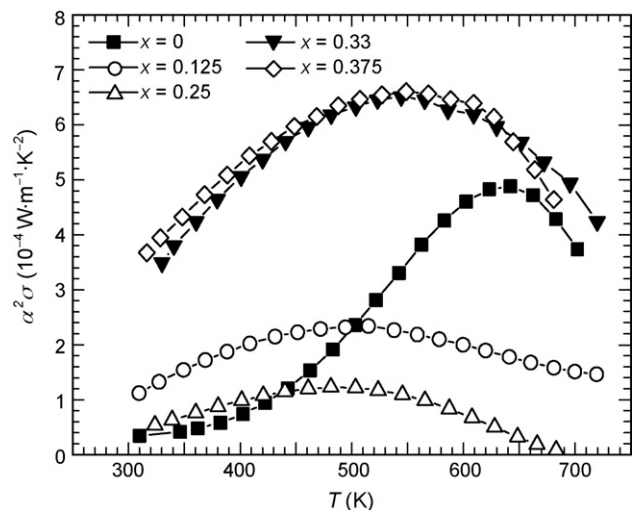


Fig. 5. Temperature dependences of power factors $\alpha^2\sigma$ for $\text{Fe}_x\text{Ni}_y\text{Co}_{1-x-y}\text{Sb}_3$.

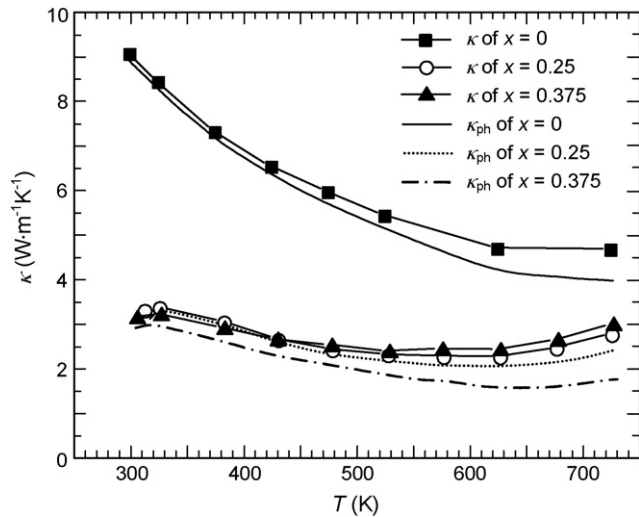


Fig. 6. Temperature dependences of thermal conductivity κ and phonon contribution κ_{ph} for $\text{Fe}_x\text{Ni}_y\text{Co}_{1-x-y}\text{Sb}_3$.

contribution κ_{ph} and the carrier contribution κ_{c} . The carrier contribution can be calculated by the Wiedemann-Franz law, $\kappa_{\text{c}} = L_0\sigma T$, where L_0 is Lorenz number. For the degenerate condition, $L_0 = 2.44 \times 10^{-8} \text{ W } \Omega \text{ K}^{-2}$ is used. The phonon contribution κ_{ph} can be obtained by subtracting κ_{c} from the total thermal conductivity κ . The temperature dependences of κ_{ph} are also shown in Fig. 6. In binary skutterudite compounds, the relatively high thermal conductivity is mainly due to the high phonon contribution. The κ_{ph} for p-type CoSb_3 was higher than 90% [12]. In the present study, it can also be seen that κ_{ph} gives a primary contribution to κ for the three samples, and the reduction of κ is mainly due to the phonon component. The substitution of Fe and Ni for Co in CoSb_3 is expected to create mass and volume disorder in the structure, which is considered as an effective way to reduce lattice thermal conductivity. One may anticipate that thermal conductivity could be further decreased if even larger mass and volume fluctuations could be achieved such as Ru and Pd substitution of Co.

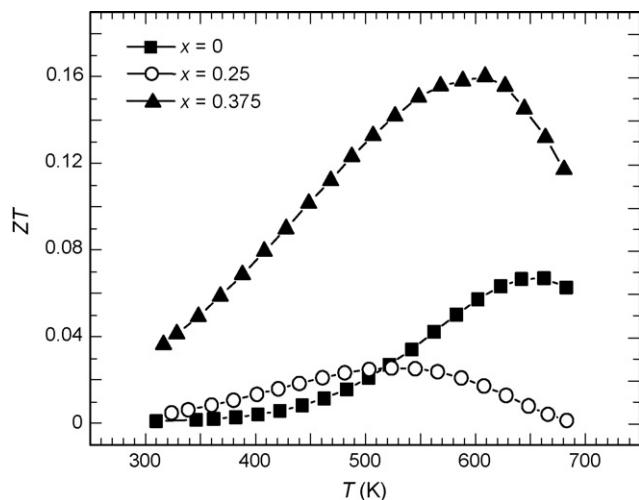


Fig. 7. Temperature dependences of the figure of merit ZT for $\text{Fe}_x\text{Ni}_y\text{Co}_{1-x-y}\text{Sb}_3$.

Fig. 7 shows the ZT values of CoSb_3 , $\text{Fe}_{0.25}\text{Ni}_{0.25}\text{Co}_{0.5}\text{Sb}_3$ and $\text{Fe}_{0.375}\text{Ni}_{0.375}\text{Co}_{0.25}\text{Sb}_3$. The ZT values increase with temperature, reach a maximum at the certain temperature, and then decrease at the higher temperatures. The temperatures at which both quaternary solid solutions reach their maximum ZT values are lower than that of CoSb_3 . The highest ZT value of 0.16 is obtained at 610 K for $\text{Fe}_{0.375}\text{Ni}_{0.375}\text{Co}_{0.25}\text{Sb}_3$. The ZT value is low compared with state-of-the-art thermoelectric materials. An optimization of the carrier concentrations might improve the thermoelectric performance for $\text{Fe}_x\text{Ni}_y\text{Co}_{1-x-y}\text{Sb}_3$ system.

4. Conclusion

Quaternary $\text{Fe}_x\text{Ni}_y\text{Co}_{1-x-y}\text{Sb}_3$ compounds were synthesized by melting the elements followed by long time annealing. Both p-type and n-type thermoelectric materials were obtained for $\text{Fe}_x\text{Ni}_y\text{Co}_{1-x-y}\text{Sb}_3$ system. The temperature dependence of electrical conductivity shows semiconductor behavior for all the samples. The values of thermal conductivity are substantially reduced by substituting Fe and Ni for Co in CoSb_3 . The maximum ZT value of 0.16 is obtained at 610 K for $\text{Fe}_{0.375}\text{Ni}_{0.375}\text{Co}_{0.25}\text{Sb}_3$, which is lower than the state-of-the-art thermoelectric materials. An optimization of the carrier concentrations might improve the thermoelectric performance for $\text{Fe}_x\text{Ni}_y\text{Co}_{1-x-y}\text{Sb}_3$ system.

Acknowledgements

This work was supported by National Basic Research Program of China (2007CB607502), Natural Science Foundation of China (50471039 and 50522203) and by the State Key Laboratory of High Performance Ceramics and Superfine Microstructure (SKL200508SIC). The authors would like to thank Dr. H. Chen, School of Materials Science and Engineering, Nanyang Technological University, for the thermal conductivity measurements.

References

- [1] T.M. Tritt, Science 283 (1999) 804.
- [2] B.C. Sales, D. Mandrus, R.K. Williams, Science 272 (1996) 1325.
- [3] D.T. Morelli, G.P. Meisner, B.X. Chen, S.Q. Hu, C. Uher, Phys. Rev. B 56 (1997) 7376.
- [4] B.C. Chakoumakos, B.C. Sales, J. Alloys Compd. 407 (2006) 87.
- [5] D. Bérardan, C. Godart, E. Alleno, E. Leroy, P. Rogl, J. Alloys Comp. 350 (2003) 30.
- [6] J.W. Sharp, E.C. Jones, R.K. Williams, P.M. Martin, B.C. Sales, J. Appl. Phys. 78 (1995) 1013.
- [7] B.C. Sales, D. Mandrus, B.C. Chakoumakos, V. Keppens, J.R. Thompson, Phys. Rev. B 56 (1997) 15081.
- [8] T. Caillat, J. Kulleck, A. Borshevsky, J.-P. Fleurial, J. Appl. Phys. 79 (1996) 8419.
- [9] G.S. Nolas, J. Yang, R.W. Ertenberg, Phys. Rev. B 68 (2003) 193206.
- [10] J.-P. Fleurial, T. Caillat, A. Borshevsky, Proceedings of the 16th International Conference on Thermoelectrics, IEEE, Dresden, 1997, p. 1.
- [11] P. Vaquero, G.G. Sobany, A.V. Powell, K.S. Knight, J. Sol. State Chem. 179 (2006) 2047.

- [12] H. Kitagawa, M. Hasaka, T. Morimura, H. Nakashima, S. Kondo, *Scripta Mater.* 43 (2000) 727.
- [13] A. Borshchevsky, T. Caillat, J.-P. Fleurial, in: *Proceedings of the 15th International Conference on Thermoelectrics, Pasadena, IEEE (1996)* 112.
- [14] D.T. Morelli, T. Caillat, J.P. Fleurial, A. Borshchevsky, J. Vandersande, B. Chen, C. Uher, *Phys. Rev. B* 51 (1995) 9622.
- [15] M. Hasaka, H. Kitagawa, K. Matano, T. Morimura, S. Kondo, *Proceedings of the 16th International Conference on Thermoelectrics IEEE, Dresden, 1997*, p. 360.